Journal of Orthopaedic Translation (2016) 5, 57—68

Available online at www.sciencedirect.com

ScienceDirect

journal homepage: http://ees.elsevier.com/jot

ORIGINAL ARTICLE

Calcium phosphate/thermoresponsive hyaluronan hydrogel composite delivering hydrophilic and hydrophobic drugs

Dalila Petta [a], Garland Fussell [b], Lisa Hughes [b], Douglas D. Buechter [b], Christoph M. Sprecher [a], Mauro Alini [a], David Eglin [a], Matteo D'Este [a,*]

[a] AO Research Institute Davos, Clavadelerstrasse 8, 7270 Davos, Switzerland
[b] DePuy Synthes Biomaterials, 1230 Wilson Drive, West Chester, PA 19380, USA

Received 5 August 2015; received in revised form 11 November 2015; accepted 17 November 2015
Available online 31 December 2015

KEYWORDS
bone graft substitute;
composite;
drug delivery;
thermoresponsive hyaluronan;
β-tricalcium phosphate

Summary *Background/Objective:* Advanced synthetic biomaterials that are able to reduce or replace the need for autologous bone transplantation are still a major clinical need in orthopaedics, dentistry, and trauma. Key requirements for improved bone substitutes are optimal handling properties, ability to fill defects of irregular shape, and capacity for delivering osteoinductive stimuli.
Materials and methods: In this study, we targeted these requirements by preparing a new composite of β-tricalcium phosphate (TCP) and a thermoresponsive hyaluronan (HA) hydrogel. Dissolution properties of the composite as a function of the particle size and polymeric phase molecular weight and concentration were analysed to identify the best compositions.
Results: Owing to its amphiphilic character, the composite was able to provide controlled release of both recombinant human bone morphogenetic protein-2 and dexamethasone, selected as models for a biologic and a small hydrophobic molecule, respectively.
Conclusion: The TCP—thermoresponsive HA hydrogel composite developed in this work can be used for preparing synthetic bone substitutes in the form of injectable or mouldable pastes and can be supplemented with small hydrophobic molecules or biologics for improved osteoinductivity.

* Corresponding author. AO Research Institute Davos, Clavadelerstrasse 8, 7270 Davos, Switzerland.
E-mail address: matteo.deste@aofoundation.org (M. D'Este).

http://dx.doi.org/10.1016/j.jot.2015.11.001

Introduction

Biomaterials able to reduce or replace the need for autologous bone transplantation are a compelling need in maxillofacial, orthopaedic, and reconstructive surgery [1]. In the context of an increasingly ageing global population that is keen on maintaining an active lifestyle and expecting improved life quality, this need is particularly urgent. Nowadays, bone grafting is a very common practice, with 2.2 million procedures being performed annually [2]. Examples of grafting procedures include spinal fusions, limb length restoration, bone reconstruction after tumour resection, and maxillary sinus augmentation [3]. In all of these and in similar cases, bone autografts are generally recognized as more effective than off-the-shelf alternatives; however, the autograft harvesting procedure is associated with considerable risks and donor site pain and morbidity, thereby lowering substantially the benefit-to-risk ratio. Therefore, calcium phosphate (CaP)-based synthetic bone graft substitutes are a valid alternative to autografts and have been clinically used for this purpose for many decades [4–6]. Despite the capacity of supporting bone ingrowth from viable bone at the grafting site (osteoconductivity), they generally do not induce bone growth *per se* (osteoinductivity). CaP-based synthetic bone graft substitutes are specifically produced with interconnected porosity, which facilitates body fluids perfusion, cell invasion, and blood vessel ingrowth. In addition, the surface chemistry of CaP is characterized by the presence of charges from calcium and phosphate ions. This feature is exploited in CaP-based drug delivery systems, particularly for genetic material [7], growth factors [8], and antibiotics [9]. For hydrophobic drug species, the ionic nature of the underlying interactions is a limitation to the versatility of CaP materials as drug delivery systems. Therefore, the combination of CaP with matrices improving their versatility as drug delivery systems is highly needed.

CaPs are generally supplied as granules of varying sizes. As with most ceramic materials, they are inherently brittle, and their mechanical strength is additionally decreased by the porosity. These are important limitations. In fact, a fundamental desirable characteristic of synthetic bone substitutes is being easily shaped to adapt to an irregular bone defect [10]. Ideally, the construct should therefore be sufficiently soft and plastic. At the same time, the implant should not be dislocated after adjacent tissue compression or body fluids washout, and therefore it should maintain its cohesion after implantation. This is often achieved by combining CaP particles and a polymeric matrix or a hydrogel [11–17].

Hydrogels are hydrated molecular networks well-known for their capability of acting as drug reservoirs and facilitating controlled drug release [18,19]. Hydrogels act as matrices, physically slowing down drug diffusion. Moreover, depending on their composition, they can establish specific chemical interactions with the drug and thereby modulate the drug release kinetics. Chemical affinity is sometimes a limitation, as non-water-soluble drugs can be difficult to incorporate into common hydrogels, which have inherently high water content. In this case, liposomes or micro/nanoparticles composites are generally used [20–22].

To target the needs of osteoconductivity, versatility, improved handling and cohesion properties, and potential drug delivery, we prepared a new combination of β-tricalcium phosphate (TCP) granules with a thermoresponsive hyaluronan (HA) matrix. In 2012, Tian et al [23] reported the use of a thermoresponsive chitosan matrix for demineralized bone matrix delivery. In our study, HA was selected as the main component because it is fully biocompatible, non-immunogenic, and readily available in medical grade. HA is a natural component of the extracellular matrix playing a key role in tissue repair [24,25]. Recently, HA was demonstrated to improve the osteoconductive properties of CaP [26]. In this study, HA was modified with pendant moieties of thermoresponsive poly(*N*-isopropylacrylamide) (pNIPAM) to obtain a co-polymer (HpN) that undergoes a temperature-induced transition to a gel state. Importantly, the transition takes place between room and body temperature without covalent cross-linking and therefore in a bio-orthogonal manner, that is, without interfering with physiological biochemical processes.

In this study, we prepared an array of TCP/HpN composites of varying TCP particle size, TCP concentration, polymer phase concentration, and molecular weight of HA within HpN and assessed their properties as potential synthetic bone grafting materials. Handling properties were determined through rheological and dissolution profiles and composites were characterized via scanning electron microscopy (SEM) imaging and micro-computed tomography (micro-CT). Selected composites were tested for their ability to act as drug delivery vehicles. Release rates from composites of recombinant human bone morphogenetic protein-2 (rhBMP-2) and dexamethasone (DEX), which were selected as models of a hydrophilic biological drug and a small hydrophobic drug, respectively, were determined. Finally, cytotoxicity against telomerase-immortalized human foreskin fibroblasts was evaluated.

Materials and methods

Materials

HA sodium salts from *Streptococcus equi* with weight-average molecular weight of 1506 kDa [high molecular weight (HMW)] and 280 kDa [low molecular weight (LMW)] were purchased from Contipro Biotech s.r.o. (Dolni Dobrouc, Czech Republic). Amino-terminated pNIPAM (number-average molecular weight, 34 kDa) was purchased from Polymer Source, Inc. (Dorval, Canada). ChronOS Beta-TCP granules with different particle sizes were supplied by DePuy Synthes USA Products LLC (West Chester, PA, USA), rhBMP-2 (InductOs; Medtronic BioPharma B.V., Heerlen, Netherlands) was purchased from Alloga AG (Burgdorf, Switzerland); DEX was purchased from TCI Europe N.V. (Zwijndrecht, Belgium); rhBMP-2 enzyme-linked immunosorbent assay (ELISA) kit Duo Set from R&D Systems Inc. (Minneapolis, MN, USA), and Cell Titer-Blue Cell Viability Assay from Promega AG (Dübendorf, Switzerland). All other reagents were purchased from Sigma–Aldrich (Buchs, Switzerland). Chemicals were of analytical grade at least, and were used without further purification.

HpN synthesis and characterization

HpN was prepared by conjugating HMW or LMW HA with amino-terminated pNIPAM via carbonyldiimidazole-mediated amide formation according to a previously described method [27] to give HHpN and LHpN, respectively.

The reaction was carried out in dimethyl sulphoxide for 2 days at room temperature and the final product was purified by dialysis against demineralized water for 5 days. HpN was freeze dried, desiccated under vacuum at 42°C, and stored at room temperature.

The molar degree of substitution (DSmol), defined as the number of carboxyl groups functionalized with pNIPAM per repeating unit of HA, was determined by ^{1}H nuclear magnetic resonance (NMR) comparing the integrals of the peaks of the non-anomeric protons of HA between 3.00 ppm and 3.77 ppm and the methyl group of the pNIPAM at 1.14 ppm. Spectra were acquired on a Bruker AVANCE AV-500 MHz NMR spectrometer. Deuterium oxide was used as a solvent and the spectra were processed using Mnova version 9.0 software (Mestrelab Research, Santiago de Compostela, A Coruña, Spain).

Rheological measurements were performed using an Anton Paar MCR-302 rheometer (Anton Paar GmbH, Baden-Wurttemberg, Germany) equipped with a Peltier temperature control device. A 25-mm diameter cone-plate geometry was used with a 0.049-mm gap, predetermined by the geometry. The freeze-dried HpN was rehydrated with a phosphate-buffered saline (PBS) solution (pH 7.4) at the desired concentration (20% w/w or 10% w/w) until homogeneity was achieved. Oscillatory tests (amplitude, frequency, and temperature sweep) were performed for each HpN sample. The linear viscoelastic region was determined using a strain sweep at a frequency of 1 Hz. A strain of 0.5% was determined to be within the linear viscoelastic region for all the HpN batches and was selected for all rheological measurements. Temperature sweep was performed between 20°C and 40°C with a ramp rate of 1°C/min at constant amplitude (0.5%) and frequency (1 Hz). Low-viscosity silicon oil was used at the meniscus interface to avoid sample drying. Figure S1 online shows the temperature sweep of 20% w/v HHpN solution.

TCP/HpN composite preparation

Composites were prepared with varying HpN polymer solution concentration, molecular weight of HA within HpN, and CaP particle content and particle size. The range of variation of each parameter is presented in Table 1. The notation used throughout this manuscript to identify a composition is as follows: the first character is either H or L, identifying high or low molecular weight of HA; the first number identifies the HpN concentration in % w/v; the second number expresses the granules content in % w/v; finally, b1, b2, b3, or b4 identifies the particle size according to Table 1. For example, the composition H20-75b4 is prepared from a 20% w/v HMW HpN solution and 75% w/v of TCP granules with a 0.7—0.14-mm size. As control, composites using pure HMW HA as polymeric phase were prepared.

To prepare the composites, lyophilized HpN and TCP particles were weighed; to this, PBS solution was added and all the components were mixed with a spatula for few minutes until a homogeneous paste was obtained.

Table 1 Range of variation of concentration and characteristics of the components within the composites.

HA M_W	HpN solution	TCP content	TCP granules size range and notation	
HMW	12% or 20%	40—80%	<0.25 mm	b1
1.5 MDa	w/v	w/v	0.25—0.5 mm	b2
LMW			0.5—0.7 mm	b3
0.28 MDa			0.7—1.4 mm	b4

HA = hyaluronan; HMW = high molecular weight; TCP = β-tricalcium phosphate; LMW = low molecular weight.

SEM imaging and micro-CT

A 100-mg bead of H20-40b2 composite was prepared, frozen in liquid nitrogen, and lyophilized. The dehydrated bead was fractured, coated with 10 nm of carbon and imaged with a Hitachi S-4700 II field emission scanning electron microscope (Hitachi High-Technologies Europe GmbH, Krefeld, Germany) at 5-kV accelerating voltage. Images were taken in the secondary electron mode. In addition, the elemental analysis of the material at the TCP/HpN interface was evaluated by energy-dispersive X-ray spectroscopy (EDX, INCA V5.2; Oxford Instruments plc, Oxfordshire, UK) with the accelerating voltage at 10 kV.

Three H20-40b1 composite beads were scanned using a μCT40 (Scanco Medical AG, Brüttisellen, Switzerland) with a resolution (voxel size) of 12 μm (70 kVp, 114 μA, and 150 ms integration time). A three-dimensional segmentation followed by a morphometric analysis was performed for the whole bead. Three spatial regions of the bead (upper, middle, and lower) consisting of 40 slices each were identified and quantitative information about the granules particle size and the distance between them were obtained.

Dissolution and injectability tests

Dissolution test

The dissolution test consists of evaluating the shape maintenance after immersion into a PBS solution at 37°C. The composite was formed into a bead and placed into a 20-mL vial filled with PBS solution at 37°C. Composites with TCP particles of size below 0.5 mm were loaded into a 1-mL syringe and extruded into a 20-mL vial filled with PBS solution at 37°C. Pictures were taken immediately after extrusion and every fifth day for 25 days.

Injectability test

Injectability of selected composites was quantitatively measured with an Instron 4302 electromechanical testing machine in compression configuration. A 0.4-mL volume of composite was placed in a 1-mL syringe with a round-tip opening of 2.1 mm inner diameter. Syringes were mounted vertically in a custom-made stand. A load cell of 50 N was

used. The compressive curve was registered at a cross-head speed of 120 mm/min. Results are reported as the average of three replicas.

rhBMP-2 and DEX release

Freeze-dried HHpN and b1 TCP granules were mixed together; a 0.1% bovine serum albumin (BSA) solution containing the drug was added and the components were mixed with a spatula for a few minutes. The formulation was shaped as a bead with a final weight of 100 mg. Beads containing rhBMP-2 (5 μg/bead) or DEX (100 μg/bead) were prepared. Control groups were HHpN bead only and TCP granules (b1) only. All control groups were loaded with the same amount of rhBMP-2 or DEX as the test samples. Samples were prepared in triplicate. Additional groups with a solution of pure rhBMP-2 or DEX were also included.

In vitro rhBMP-2 release

rhBMP-2 was supplied as a lyophilized powder in a formulation buffer containing 2.5% glycine, 0.5% sucrose, 0.01% polysorbate 80, 5mM sodium chloride, and 5mM L-glutamic acid. The protein was reconstituted to a final concentration of 1.5 mg/mL in a 0.1% BSA solution in PBS and then with the formulation buffer supplemented with 0.1% BSA, to a final concentration of 500 μg/mL. For the release study, 10 μL of this solution was added to the polymeric phase during the preparation of the composite bead to load each sample with 5 μg of rhBMP-2. A release experiment was performed under the same conditions except for loading the growth factor in the inorganic phase. The release of rhBMP-2 from the composite was determined by placing each composite bead in 1 mL of release buffer (PBS + 0.1% BSA + 0.05% sodium azide) in low protein-binding Eppendorf tubes at 37°C under mild agitation (10 rpm). At different time points (1 hour, 3 hours, 8 hours, 1 day, 2 days, 3 days, 5 days, 8 days, and 13 days), 100 μL of release buffer was withdrawn and replaced with the same amount of fresh buffer. Samples were stored at −20°C until ELISA analysis. The ELISA was run after appropriate dilution following the protocol provided by the supplier and the final absorbance was measured at 450 nm and corrected with the reading at 540 nm for optical compensation. The concentration of rhBMP-2 released from the different samples was normalized to the actual rhBMP-2 detected in the control group (5 μg of rhBMP-2 in release buffer). The tested items were prepared in triplicate and each replica was run in duplicate for the ELISA. Final concentrations were calculated according to the dilution at every time point.

Sodium dodecyl sulphate-polyacrylamide gel electrophoresis

Sodium dodecyl sulphate-polyacrylamide gel electrophoresis (SDS-PAGE) was performed to detect the rhBMP-2 that was not released from the TCP granules. Samples analysed were as follows: (1) 5 μg/mL rhBMP-2 as control, reconstituted with or without 0.1% BSA and (2) TCP granules loaded with 5 μg of rhBMP-2 after 13 days of incubation in release media.

Samples (1) and (2) were tested under reducing (β-mercaptoethanol) and nonreducing conditions by incubating for 5 minutes at 95°C in Laemmli buffer, consisting of 62.5mM Tris—HCl (pH 6.8), 25% glycerol, 2% SDS, and 0.01% bromophenol blue. TCP granules from Sample (2) were removed from the release media before addition to the Laemmli buffer. Samples were loaded on a 15% gel and the electrophoresis was run at 100 V for 20 minutes and then at 80 V for an additional 1 hour and 30 minutes. The gel was stained with a coomassie blue G-250 for 20 minutes (coomassie blue 0.3% + acetic acid 10% + methanol 25%) and destained in methanol/acetic acid solution (25% methanol + 10% acetic acid). Destained gels were visualized using the ChemiGenius Bioimaging System (Syngene, A Division of Synoptics Ltd, Cambridge, United Kingdom).

In vitro DEX release

DEX was freshly reconstituted with ethanol to a concentration of 5 mg/mL. DEX solution (20 μL) was loaded onto TCP b1 granules. The solvent was allowed to evaporate at room temperature and HpN + PBS was added to obtain 100 μg of DEX for each bead. For the release study, each composite bead was incubated at 37°C under mild agitation conditions in 1.5 mL of release buffer. The release was carried out for 13 days and for each time point, 300 μL of release buffer was removed and replaced with fresh buffer. Collected samples were stored at 4°C until analysis. DEX was quantified by high-performance liquid chromatography on a Kinetex 5-μm C_{18} 100A column (Phenomenex Inc., Torrance, CA, USA) with triamcinolone acetonide as internal standard [28]. Mobile phase was acetonitrile:water 28:72, pH 2.3, at a flow rate of 1.2 mL/min and the detector wavelength was 241 nm. In a set of six replicates of the same sample, a standard deviation of 1.6% was found (data not shown). The linearity of the DEX was between 0.35 μg/mL and 12.5 μg/mL. Final concentrations were calculated according to the dilution at every time point. Furthermore, the specimens were allowed to release for up to 3 months, following which they demonstrated no further release (data not shown).

Reconstitution time of dry formulations

Reconstitution of the formulation H20-40b1 was performed using two different protocols, identified as A and B. In Protocol A (see Video S1 online), the ceramic and the polymeric phase of the composite were mixed and rehydrated with a 500 μg/mL rhBMP-2 solution. In Protocol B, the composite was prehydrated with a 500 μg/mL rhBMP-2 solution and weighed. MilliQ water was added, which results in a threefold weight increase. The bead was smashed with a spatula and freeze dried. Finally, the freeze-dried composite formulation was reconstituted to its original volume (before swelling to the threefold weight increase) with MilliQ water (see Video S2 online). For both Protocols A and B, the reconstituted material had the following composition: 98 mg of TCP granules (b1), 50.4 mg of HpN, 35 μL of rhBMP-2 solution (500 μg/mL), and 217 μL of PBS solution. For both protocols, reconstitution was performed in a plastic vessel by mixing manually with a spatula.

Supplementary data related to this article can be found online at http://dx.doi.org/10.1016/j.jot.2015.11.001.

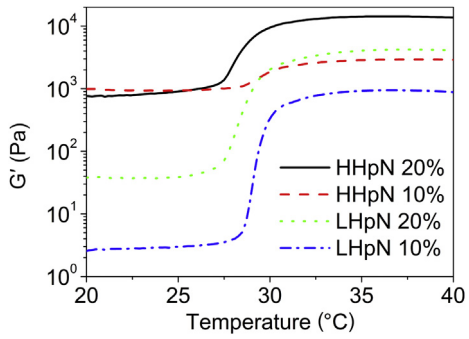

Figure 1 Storage modulus G′ against the temperature of 20% w/v (black line) and 10% w/v (red dashed line) HHpN and 20% w/v (green dotted line) and 10% w/v (blue dash—dot line) LHpN solutions.

Cytotoxicity assay of the composite formulation

Cytotoxicity was evaluated by assessing the viability of telomerase-immortalized human foreskin (hTERT-BJ1) fibroblasts after contact with extracts of composite beads. A CellTiter-Blue Cell Viability Assay (Promega AG) was performed in conformity to the ISO STANDARD 10993-5. The tested substances were sterilized with cold ethylene oxide. All the samples were incubated for 24 hours in 2.5 mL of extraction vehicle at 37°C, that is, culture medium supplemented with 5% foetal calf serum and either 0.5 g of the composite—15 cm^2 of the positive control (latex)—or 7.5 cm^2 of the negative control (high-density polyethylene). hTERT-BJ1 fibroblasts were seeded in 96-well plates at a density of 2000 cells/100 μL of culture medium (Dulbecco's modified Eagle's medium supplied with 5% foetal calf serum) in a 96-well plate and incubated for 24 hours at 37°C, 5% CO_2, 95% humidity. The medium was then removed from each well and 100 μL of the different extraction media from the test items were added to each well in triplicate. On Days 1 and 3, the extraction medium was removed and cells were incubated with a 10% CellTiter-Blue solution for 2.5 hours. The fluorescence signal was read using a VICTOR3 Perkin Elmer plate reader (Perkin Elmer Inc., Waltham, MA, USA). All fluorescence values were normalized to the fluorescence value of the cells seeded in the presence of culture medium at Day 1 and Day 3.

Results

Characterization of the co-polymer

HpN co-polymers with different rheological properties were synthesized according to protocols already established [27]. DSmol of HpN was consistently 5% of the carboxyl groups functionalized, corresponding to about 9 mol of pNIPAM/mole of HA repeating unit. The temperature dependence of the storage modulus of HpN solutions of high and low molecular weight at 10% w/v and 20% w/v concentration is shown in Figure 1. LHpN at 10% w/v showed a sharp transition

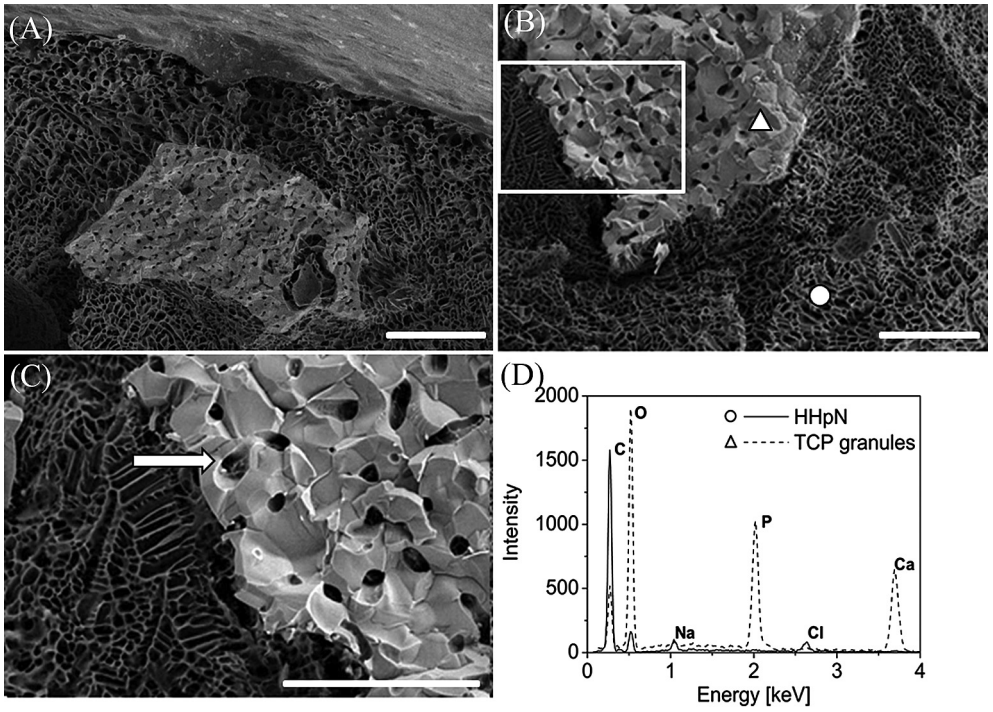

Figure 2 Scanning electron microscopy images of an H20-40b2 bead cross section. (A) Interface between the external surface and the bulk of the bead, where a β-tricalcium phosphate (TCP) granule completely embedded in hydrogel is visible. (B) Bulk of another area within the same specimen. The white rectangular frame is magnified in panel (C), where the white arrow indicates hydrogel within a TCP pore. The white triangle on the TCP and circle on the hydrogel in panel (B) represent the focal regions where energy-dispersive X-ray spectroscopy spectra in panel (D) were acquired. All scale bars correspond to 50 μm.

around 29°C, with the storage modulus increasing over two orders of magnitude between room temperature and physiological temperature. At 20% w/v concentration, the LHpN storage modulus was 10-fold higher than LHpN at 10% w/v and showed a fivefold increase as the temperature was increased from room temperature to physiological temperature with a slight decrease in the transition temperature at the higher concentration. G′ of HHpN was markedly higher than LHpN at room temperature at both 10% w/v and 20% w/v, and the transition amplitude was smaller, especially for HHpN 10% w/v.

An evaluation of the formulation stability of 20% w/v HHpN was carried out by measuring the rheological profile at different time points out to 11 weeks. Results in Figure S1 online show how the temperature-induced sol–gel transition and viscoelastic shear moduli values were maintained.

SEM and micro-CT imaging of the composites

Figure 2A shows the cross section of a fractured bead of the composite H20-40b2. The external surface of the bead in the upper part of the image is visible as a smooth layer, under which the dried hydrogel shows a porosity of characteristic size around 5 μm. A TCP granule embedded in the hydrogel matrix is clearly visible as a denser and brighter area. Figures 2B and 2C represent another area from the same sample. The gapless contact between the hydrogel and the ceramic surface is obvious, with the hydrogel filling the macroporosity as well as the microporosity within the TCP granules (Figure 2C and Figure S2). Results of EDX spectroscopy showed the presence of carbon, oxygen, phosphorus, and calcium for the mineral part and carbon, oxygen, sodium, and chloride for the hydrogel part (Figure 2D).

The three-dimensional segmentation analysis from micro-CT imaging confirmed the uniform distribution of TCP granules within the HpN polymeric matrix, both on the surface and inside the bead, as shown in Figure 3A.

The morphometric analysis for the whole volume of the bead (Figure 3B) displayed a Gaussian distribution of the granules size, expressed as particle thickness (Figure 3C). Furthermore, the mean granules distance (Figure 3D) in the three different regions U, M, and L was 0.225 mm, 0.209 mm, and 0.197 mm, respectively (standard deviation 6.63%).

Dissolution and injectability test

The results of the dissolution test of formulations prepared with varying content of hydrogel and inorganic phase are reported in Table 2.

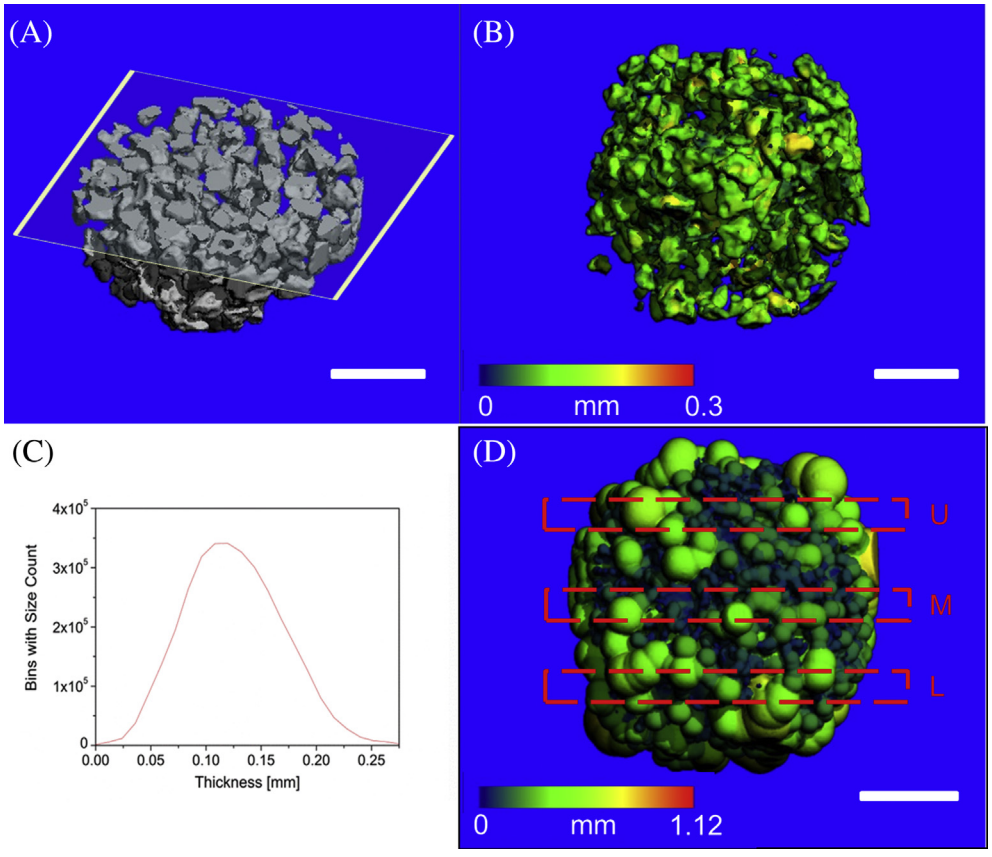

Figure 3 Micro-computed tomography scan of the H20-40b1 composite. (A) Three-dimensional reconstruction of half bead section; (B) size distribution of the β-tricalcium phosphate (TCP) granules within the composite (the gradient colour bar indicates the thickness in mm); (C) distribution of the particle size after a two-point fast Fourier transform filter smoothing; (D) spatial distribution of the TCP granules (the gradient colour bar indicates the distance between the granules in mm, the red dashed rectangles indicate the three analysed regions, namely, upper (U), middle (M), and lower (L). Scale bars = 1 mm.

Table 2 Outcome of the dissolution test.

Abbreviation	Dissolution test
HA HMW 20% + 60% b3	Not passed
H20-40b1	Passed
H20-40b2	Passed
H20-40b3	Passed
H20-40b4	Passed
H20-60b3	Passed
H20-80b3	Passed
H20-80b4	Passed
L12-50b3	Not passed
L12-60b3	Not passed
L12-80b1	Not passed
L12-75b2	Not passed
L12-80b3	Partially passed
L20-40b1	Partially passed
L20-40b2	Partially passed
L20-40b3	Partially passed
L20-60b3	Partially passed
L20-80b3	Partially passed
L20-40b4	Passed
L20-60b4	Passed
L20-80b4	Passed

Nomenclature of abbreviations in Table 2 is explained in the "TCP/HpN Composite Preparation" section.
HA = hyaluronan; HMW = high molecular weight.

Putties prepared from HHpN at 20% w/v (H20-40b1, H20-40b2, etc.) passed the dissolution test for each granule size and concentration of mineral phase tested. These composites displayed shape maintenance, no turbidity, and no crumbling of the particles for 25 days, as shown in Figure 4B. These samples were stored for 8 months in the same conditions and showed no visible changes (data not shown). The putty prepared from pristine HMW HA at the same concentration (first row in Table 2) disintegrated completely after dissolution testing (see Figure S3 online). Dissolution tests of LHpN putties gave results dependent on both polymer concentration and particle size. Formulations prepared from LHpN at 12% w/v showed a relatively low viscosity for paste preparation and gave negative outcome for all particles content, except for the dissolution test of the sample L12-80b3, where the shape was maintained and only a few particles detached (see Figure S4 online). Therefore, for this sample, a partial pass was attributed. Increasing the LHpN concentration to 20%, w/v formulations showed a visible shape collapse in the dissolution test (see Figure S5 online). Because the basic shape was maintained and very minor particle crumbling was observed, this was considered a partial pass (Figure 4A). Putties prepared from b4 particles (size 0.7–1.4 mm) and LHpN 20% w/v, fully passed the test.

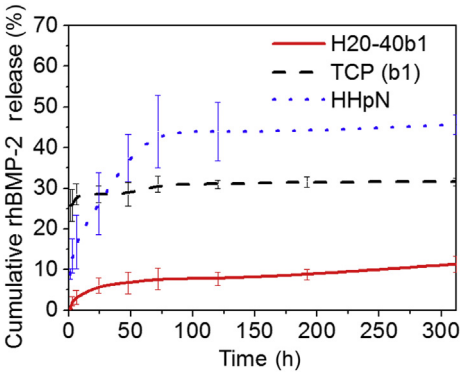

Figure 5 Cumulative release of recombinant human bone morphogenetic protein-2 (rhBMP-2) from the H20-40b1 composite (red solid line), from HHpN (blue dotted line), and from β-tricalcium phosphate (TCP) granules (black dashed line). Values are normalized to the total loaded. The lines represent the average of three replicas and the bars the standard deviation.

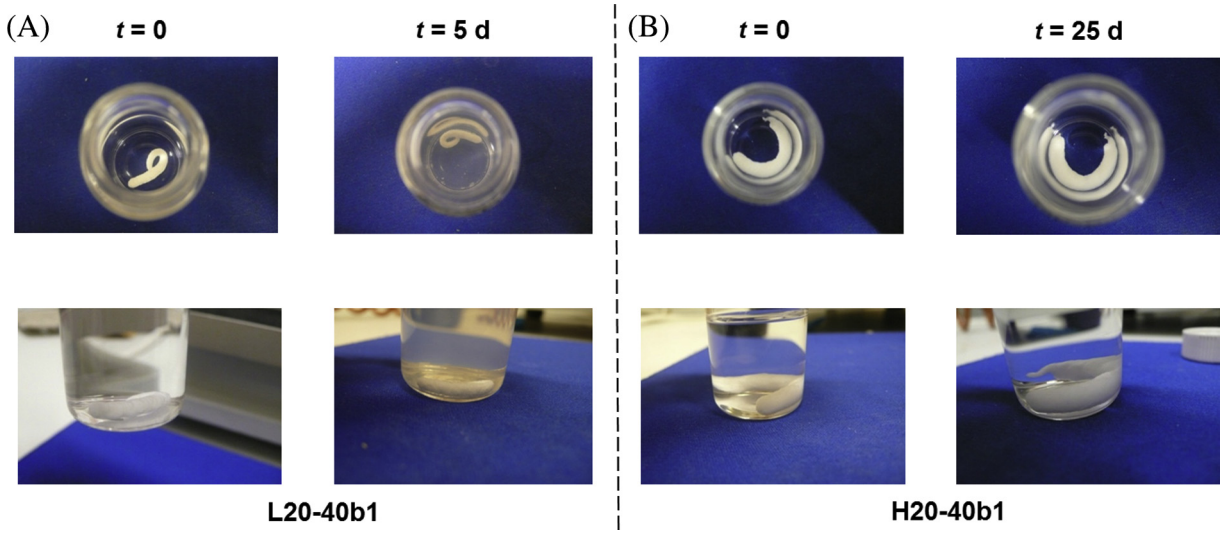

Figure 4 Dissolution test for the composites. (A) L20-40b1 at time (*t*) 0 days and 5 days and (B) H20-40b1 at time (*t*) 0 days and 25 days.

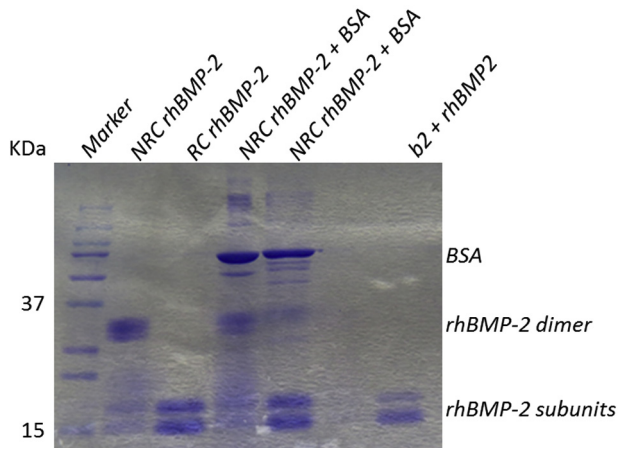

Figure 6 Sodium dodecyl sulphate-polyacrylamide gel electrophoresis of recombinant human bone morphogenetic protein-2 (rhBMP-2) reconstituted in the presence (Lanes III and V) or absence (Lanes II and IV) of β-mercaptoethanol. Lane VI contains β-tricalcium phosphate (TCP) granules loaded with 5 μg of rhBMP-2; Lane I corresponds to the markers solution (Precision Plus Protein Western C Standard). BSA = bovine serum albumin.

Injectability

The extrusion of the composites with granules of size above 0.5 mm led to the creation of a composition gradient with the extruded part enriched in polymeric phase and smaller particles, and the retained material enriched in the TCP solid phase. This phenomenon is known as *filter pressing*, *phase migration*, or *phase separation* [29—31]. Compositions with particles below 0.5 mm were extruded without visually observable filter pressing. Based on this outcome, only composites containing TCP granules of particle size below 0.5 mm were further developed as injectable formulations.

A quantitative injectability testing was performed in triplicate for the H20-40b2 formulation, prepared from the highest concentration of the HMW polymer with the biggest particle size suitable for injection. The force—displacement profiles were characterized by a rapid increase of the force at the beginning of the extrusion and a transition to a smooth plateau phase (see Figure S6 online). The extrusion force is in a very low range for the investigated formulation, with a plateau around 4 N.

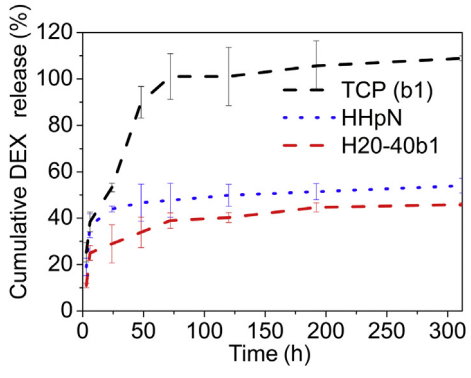

Figure 7 Curves of cumulative release of dexamethasone (DEX) from the H20-40b1 composite (dashed red line), from HHpN (dotted blue line), and from b1-TCP (solid black line). The data represent the average of three replicas and the bars the standard deviation. TCP = β-tricalcium phosphate.

rhBMP-2 release

In Figure 5, the release profile of rhBMP-2 is displayed. Pure HHpN hydrogel (blue dotted line) released most of the available rhBMP-2 in the first 3 days. TCP granules displayed a burst release achieving most of the amount obtainable over the 300-hour period released within the first 6 hours (black dashed line). For the H20-40b1 composite, the release was more controlled, with lower amounts released for each time point (red solid line) compared with either TCP granules or HpN. The fraction of rhBMP-2 released over the study compared with the nominal loaded amount was 45% for HHpN, 30% for TCP b-1, and 10% for the composite.

rhBMP-2 remaining on the TCP particles after the release study was analysed via SDS-PAGE. In Figure 6, Lanes II—V are rhBMP-2 at 5 μg/mL, whereas Lane VI represents the analysis of the TCP particles after the release study. rhBMP-2 under nonreducing conditions (Lane II) gave a band at molecular weight of approximately 30 kDa, as expected. In reducing conditions (Lane III), rhBMP-2 was split into two major subunits of approximately 15 kDa. In Lanes IV (nonreducing) and V (reducing), the same analysis was performed in the presence of BSA, confirming the previous results and showing an intense band from BSA at approximately 66 kDa, as expected. The analysis of the TCP particles under reducing conditions after extraction for 13 days (Lane VI) clearly demonstrated the split of rhBMP-2 into its monomeric units. BSA was not detectable for this sample.

Reconstitution of dry formulations

Reconstitution of the dry formulations was performed to obtain composites containing rhBMP-2, and is shown in Supplementary Videos S1 and S2 online for Protocols A (reconstitution with rhBMP-2 solution) and B (reconstitution with water, rhBMP-2 included in the dry phase), respectively. Regardless of the protocols used, after around 1.5 minutes, the formulation reached a grade of homogeneity sufficient for further use and could be handled and shaped as a bead. A small amount of adhesion of the composite to the plastic vessel was noted.

DEX release

Figure 7 compares the release of DEX from the H20-40b1 composite and from its components TCP (b1) and HHpN. TCP released 38% of DEX after 3 hours and 53% after 6 hours. HHpN and H20-40b1 did not display such a substantial burst, with 44% and 29% released at 6 hours, respectively. The composite exhibited a lower burst release and a more gradual extended release compared with HHpN. At the end of the study, 47% of the loaded DEX was released from H20-40b1. Compared with rhBMP-2, for both HpN and

the composite, the release of rhBMP-2 was slower compared with the DEX release. At 24 hours, TCP particles released 90% of DEX. In the same conditions, rhBMP-2 was released to an amount of 28% of the total load. For both rhBMP-2 and DEX, the amount released after 24 hours followed the order TCP > HHpN > composite.

Cytotoxicity

At 24 hours, the H20-40b2 composite extract showed a cytotoxicity of 25%; after 72 hours the cytotoxicity was 19%. Extracts of TCP granules alone were not cytotoxic at any time point (Figure 8). According to the ISO 10993—5:2009 standard, the threshold deemed cytotoxic is viability below 70%, or cytotoxicity above 30%. The polyethylene extract at 72 hours gave fluorescence signal higher than the control (hTERT-BJ1 + medium), which indicates a possible proliferation of the cells in these conditions.

Discussion

Characterization and general properties

Chemical modification of HA with amphiphilic moieties of pNIPAM provides this semisynthetic derivative with the singular feature of inducing a sharp transition to a gel state and an increase of viscoelastic shear moduli of more than two orders of magnitude within a narrow temperature interval. The reciprocal influence of the molecular weight of the polymeric components, relative degree of substitution, and concentration were previously analysed [32]; the system was optimized for a sharp transition and negligible shrinking [33].

In this study, we prepared and characterized a wide spectrum of composites of varying molecular weight of HA

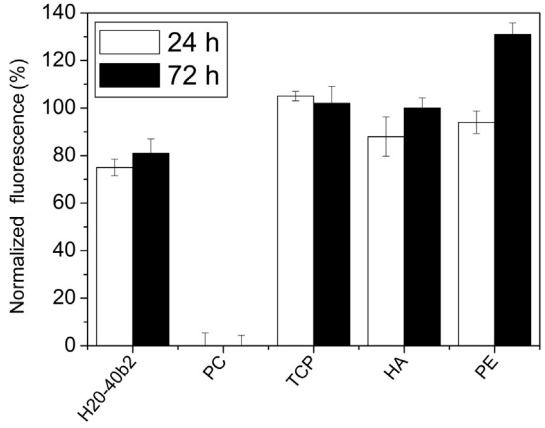

Figure 8 Values of fluorescence obtained from alamarBlue assay for pure extracts of the composite H20-40b2, β-tricalcium phosphate (TCP) granules, and hyaluronan (HA) after incubation of hTERT-BJ1 fibroblasts with extraction medium at 24 hours (white bars) and 72 hours (dark bars), respectively. PC and PE represent, respectively, the positive control (latex) and the negative control (high-density polyethylene). The error bars represent the standard deviation in percentage calculated on a number of three repeats.

within HpN, total concentration of polymer, total content of TCP particles, and TCP particle size. Composites were characterized for their shape retention after incubation in buffer. This testing is designed to challenge the composite's capability of holding together in humid environment and thereby mimic the conditions after implantation. Pristine HA is known for its extremely high hydrophilicity. Therefore, the composite prepared from pure HA (HA HMW 20% + 60% b3, control) was easily swollen in water and fell apart during dissolution testing. By contrast, composites prepared from 20% w/v HHpN were able to maintain their shape owing to the underlying molecular network and gel properties. The LHpN solution at 12% w/v concentration did not have adequate cohesiveness and at least a 20% w/v concentration of the polymer in the composite was required for displaying some degree of shape retention. This was expected, because for the polymer to act as a binder for the particles, it must be sufficiently viscous. For the same reason, HHpN gives better performance compared with the LHpN. Temperature sweep analysis shows that HHpN displays higher moduli at both room and body temperature. Specifically, the increased viscosity at room temperature gives a better initial cohesion to the composite and makes it more easily handled. Formulations prepared from 20% w/v LHpN had rheological properties barely sufficient to bind the particles, and therefore the outcome of the dissolution test was particle size dependent, with only the bigger particles giving satisfactory cohesion. Micro-CT analysis is a powerful tool for evaluating particle size and distribution within the composites. Particle size analysis confirmed the expected dimension, revealing no particle coalescence. Particle distribution was relatively uniform throughout the bead with no evidence of significant sedimentation. SEM images show a gapless contact between the ceramic granules and the polymeric matrix, with the hydrogel penetrating the microporosity (Figure 2C and Figure S2 online). The local composition assessed by EDX analysis confirmed the identification of the components. The carbon in the bioceramic part arises from the carbon coating, whereas chlorine results from the PBS as solvent for the HpN. The sodium is derived from both the PBS and as counterion for the carboxyl groups of HA.

Intuitively, improving the cohesion of a formulation works to the detriment of injectability. It is known that the force versus displacement curves characterize the extrusion process and depend on syringe size and type, plunger displacement speed, material and gauge of cannula as well as the rheological properties of the ceramic particles [11]. The extrusion test showed that the composites H20-40b1 and H20-40b2 can be extruded from an insulin syringe with a very little force and without phase separation, whereas formulations with granules above 0.5 mm exhibit filter pressing. Therefore, the composites with particle size below 0.5 mm are suitable for the preparation of both mouldable putties and injectable formulations, whereas composites with particle size above 0.5 mm are suitable for the preparation of mouldable putties. The form in which a composite biomaterial is provided to the surgeon is important for its clinical performance [34]. The HpN copolymer maintains its temperature-induced gel-formation performance for at least 11 weeks upon storage in solution at 4°C. This stability allows the preparation of the

composites as off-the-shelf prehydrated formulations. As shown in the Supplementary Videos S1 and S2 online, rehydration of the dry form immediately before use is also possible within a time span conveniently compatible with surgical procedures. Therefore, the composites presented in this study are suitable for the preparation of both prehydrated and to-be-reconstituted formulations.

The degradation profile of the composites here presented is governed by the degradation of its components. For TCP, the resorption is mainly cell mediated [35]. The polymeric carrier is subject to enzymatic degradation *in vitro* [33] and *in vivo* [36]. Therefore, the degree of chemical modification on HA in the thermoresponsive gel is such that the derivative is still recognized by hyaluronidase, which is indicative of preservation of HA biological activity. Unlike HA, pNIPAM is not biodegradable. However, *in vivo* it is eliminated via urinary excretion [37]. This fate is similar to polyethylene glycol, which is widely used in biomaterials and pharmaceutical preparations for parenteral use [38].

rhBMP-2 and DEX release

Ideally, biomaterial-based delivery systems are intended to enhance the natural tissue response by supplying adequate biochemical cues. Bone healing entails a complex cascade of events, progressing under the regulation of different small and biological molecules. In this study, we selected rhBMP-2 and DEX as model molecules to deliver. rhBMP-2 is a water-soluble full-size protein of molecular weight 30 kDa and an isoelectric point of approximately 9 and is well-known for its bone-inducing properties [39,40]. rhBMP-2 delivered in absorbable collagen sponge is already approved for clinical use in spine fusions [41] and tibial fractures [42]. DEX (molecular weight = 392.46 Da) is a non-water-soluble synthetic steroidal anti-inflammatory drug that was selected as a model for small hydrophobic molecule. Although typically used in cell culture as component of osteogenic media, DEX is not clinically used for bone growth. The molecules selected have different physicochemical properties, and were deemed suitable for assessing the versatility of a delivery system. Based on the injectability, the composite H20-40b1 was selected for performing rhBMP-2 and DEX release studies.

To accomplish its therapeutic action, rhBMP-2 needs to be released at the appropriate dose and time [43]. The potency of rhBMP-2 in inducing bone is well recognized, but after years of clinical use, serious issues of efficacy and safety have been posed [44—46]. Most of these issues arise from a suboptimal delivery system, which releases high doses of rhBMP-2 over a short period. The composite presented in this study was effective in slowing down the release of rhBMP-2, as shown in Figure 5, compared with HpN or TCP alone. The dose of rhBMP-2 released was previously demonstrated to be effective in inducing bone regeneration *in vivo* without ectopic bone formation or other side effects [47]. The comparison of rhBMP-2 and DEX release highlights that (1) TCP releases almost immediately most of the 100 μg of DEX loaded, whereas only 30% of the 5 μg of rhBMP-2 loaded is released with a quasi-zero-order kinetics; (2) HHpN and H20-40b1 show similar release kinetics for DEX, but a quite different profile for rhBMP-2, for which HHpN reaches plateau after 3 days, but the composite displays a more gradual release; and (3) the total and relative amounts released over the study are higher for DEX. These differences emphasize how the release is molecule dependent. The affinity of rhBMP-2 for CaP surfaces is known [48,49]. rhBMP-2 was still detectable on the TCP particles after the release study through SDS-PAGE. Interestingly, BSA, which was present in significant amount in the release medium, was not detected on the particles, indicating specificity of the TCP—proteins interaction. The high retention of rhBMP-2 observed for the HpN/TCP composite is not expected after implantation *in vivo*. *In vitro* release models do not mimic the tissue environment, body movements generating mechanical forces, blood and lymphatic circulation, the enzymatic degradation or the action of inflammatory cells, and the resorption of TCP by osteoclasts. Therefore, *in vivo* the total amount of rhBMP-2 released is expected to be closer to the loaded dose, as previously reported [20]. A limitation of this study is that the biological activity of BMP-2 after the release was not assessed. However, BMP-2 was identified via ELISA. If the BMP-2 structure was compromised during encapsulation and release, BMP-2 would not be able to present the epitope to the ELISA. Therefore, the positivity of the released BMP-2 to ELISA is an indication of structure preservation. The optimal pharmacokinetic of rhBMP-2 can only be determined in an *in vivo* model, and its determination needs to be investigated in future studies [50].

In contrast to rhBMP-2, DEX shows low affinity to the mineral phase and its release from TCP is quantitative, whereas HpN retains 40% of DEX. The combination of TCP with HpN induces a more gradual release (Figure 7). In our model, the release of DEX is at least in part due to dissolution, as its concentration is above the solubility threshold. Similar to TCP, HA is hydrophilic and scarcely suitable to generate hydrophobic interactions capable of modulating the release of hydrophobic species like DEX. However, in our research, we used HA modified with moieties of pNIPAM. Therefore, the use of a carrier constituted by HA chemically modified with pNIPAM provides two fundamental benefits: (1) providing the property of temperature-induced gelation, which gives good injectability but at the same time no dissolution in physiological conditions, as verified via dissolution test and (2) introducing hydrophobic domains into the HA backbone; besides forming a molecular network at body temperature, these hydrophobic domains can interact with hydrophobic species like DEX modulating its release. Understanding the association of drug molecule with composite components, as well as the effect of polymer and inorganic ratios and properties on drug incorporation and release provides the option for tailored drug delivery based on clinical need.

Conclusion

In this study, we introduced a new synthetic bone substitute composed of TCP and a thermoresponsive HA hydrogel. The co-polymer has a low degree of derivatization, and therefore it should be readily recognized as natural

extracellular matrix component by the host tissue. Owing to the temperature-induced sol—gel transition of the soft polymeric phase, handling properties are superior compared with pristine HA composites in terms of cohesion and dissolution. The composite displays good cohesion in aqueous solution at physiological temperature and osmolarity, indicating the capability of filling defects of irregular shape without washing out. Depending on the particle size, putty or injectable formulations can be prepared. rhBMP-2 and DEX were selected as models of hydrophilic full-size protein and small hydrophobic molecule to be released from the composite, demonstrating the possibility of releasing a wide range of molecules in a controlled manner. The composite contains ionically charged surfaces, hydrophilic, and amphiphilic functional groups. The interaction of these microdomains with a drug will result in different release characteristics for different molecules. For rhBMP-2, the strong interaction with the bioceramic results in a slower release and at the same time a lower overall recovery *in vitro*, compared with DEX. The capability of releasing drugs of different nature in a controlled manner is relevant towards the translation of synthetic bone graft substitutes in clinical use. Bone grafting is used in a variety of clinical situations, including, for example, bone reconstruction after trauma, deformity or tumour resection, sinus augmentation after tooth extraction, or spinal fusion in elderly or younger patients. A versatile off-the-shelf synthetic graft could be supplemented by the surgeon with different drugs, for example, angiogenic stimuli, osteoinductive stimuli, anti-inflammatory, analgesic, antibiotic, anticancer drugs depending on the clinical necessity. The composite can be supplied as both a dry formulation to be reconstituted perioperatively or as a ready-to-use paste. Owing to its handling, cohesion, resistance to washout, drug-delivery properties, and cytocompatibility, HpN/TCP composites are promising substitutes for autologous bone transplantation in orthopaedics, dentistry, and trauma.

Conflicts of interest

Garland Fussell, Lisa Hughes, and Douglas D. Buechter are employees of DePuy Synthes or were employees of DePuy Synthes when the experimental work was designed and performed.

Funding/support

The work here presented received partial support from DePuy Synthes Biomaterials; precisely, the TCP particles were provided by DePuy Synthes Biomaterials and Dalila Petta's internship was sponsored by DePuy Synthes Biomaterials.

Acknowledgements

The authors would like to acknowledge Mr Markus Glarner and Mr Dieter Wahl of the AO Research Institute for their excellent technical assistance.

Appendix A. Supplementary data

Supplementary data related to this article can be found at http://dx.doi.org/10.1016/j.jot.2015.11.001.

References

[1] Yuan H, Fernandes H, Habibovic P, de Boer J, Barradas AM, de Ruiter A, et al. Osteoinductive ceramics as a synthetic alternative to autologous bone grafting. Proc Natl Acad Sci USA 2010;107:13614—9.
[2] Giannoudis PV, Dinopoulos H, Tsiridis E. Bone substitutes: an update. Injury 2005;36:S20—7.
[3] Stiller M, Kluk E, Bohner M, Lopez-Heredia MA, Muller-Mai C, Knabe C. Performance of beta-tricalcium phosphate granules and putty, bone grafting materials after bilateral sinus floor augmentation in humans. Biomaterials 2014;35:3154—63.
[4] Johnson KD, Frierson KE, Keller TS, Cook C, Scheinberg R, Zerwekh J, et al. Porous ceramics as bone graft substitutes in long bone defects: a biomechanical, histological, and radiographic analysis. J Orthop Res 1996;14:351—69.
[5] Hirata M, Murata H, Takeshita H, Sakabe T, Tsuji Y, Kubo T. Use of purified beta-tricalcium phosphate for filling defects after curettage of benign bone tumours. Int Orthop 2006;30:510—3.
[6] LeGeros RZ. Calcium phosphate-based osteoinductive materials. Chem Rev 2008;108:4742—53.
[7] Kingston RE, Chen CA, Okayama H. Calcium phosphate transfection. In: Coligan JE, Kruisbeek AM, Margulies DH, Shevach EM, Strober W, editors. Current protocols in immunology. New York: Greene Publishing and Wiley-Interscience; 2001. 10.13.1—10.13.9.
[8] Bose S, Tarafder S. Calcium phosphate ceramic systems in growth factor and drug delivery for bone tissue engineering: a review. Acta Biomater 2012;8:1401—21.
[9] Ginebra MP, Traykova T, Planell JA. Calcium phosphate cements: competitive drug carriers for the musculoskeletal system? Biomaterials 2006;27:2171—7.
[10] Daculsi G. Smart scaffolds: the future of bioceramic. J Mater Sci Mater Med 2015;26:154.
[11] Heinemann S, Rössler S, Lemm M, Ruhnow M, Nies B. Properties of injectable ready-to-use calcium phosphate cement based on water-immiscible liquid. Acta Biomater 2013;9:6199—207.
[12] Mickiewicz RA, Mayes AM, Knaack D. Polymer—calcium phosphate cement composites for bone substitutes. J Biomed Mater Res 2002;61:581—92.
[13] Alkhraisat MH, Rueda C, Marino FT, Torres J, Jerez LB, Gbureck U, et al. The effect of hyaluronic acid on brushite cement cohesion. Acta Biomater 2009;5:3150—6.
[14] Bigi A, Bracci B, Panzavolta S. Effect of added gelatin on the properties of calcium phosphate cement. Biomaterials 2004;25:2893—9.
[15] Liu W, Zhang J, Weiss P, Tancret F, Bouler JM. The influence of different cellulose ethers on both the handling and mechanical properties of calcium phosphate cements for bone substitution. Acta Biomater 2013;9:5740—50.
[16] D'Este M, Eglin D. Hydrogels in calcium phosphate moldable and injectable bone substitutes: sticky excipients or advanced 3-D carriers? Acta Biomater 2013;9:5421—30.
[17] Barbieri D, Yuan H, de Groot F, Walsh WR, de Bruijn JD. Influence of different polymeric gels on the ectopic bone forming ability of an osteoinductive biphasic calcium phosphate ceramic. Acta Biomater 2011;7:2007—14.
[18] Gong C, Qi T, Wei X, Qu Y, Wu Q, Luo F, et al. Thermosensitive polymeric hydrogels as drug delivery systems. Curr Med Chem 2013;20:79—94.

[19] Vashist A, Vashist A, Gupta YK, Ahmad S. Recent advances in hydrogel based drug delivery systems for the human body. J Mater Chem B 2014;2:147—66.
[20] Chung YI, Ahn KM, Jeon SH, Lee SY, Lee JH, Tae G. Enhanced bone regeneration with BMP-2 loaded functional nanoparticle-hydrogel complex. J Control Release 2007;121:91—9.
[21] Schwendener RA, Schott H. Liposome formulations of hydrophobic drugs. Methods Mol Biol 2010;605:129—38.
[22] Trimaille T, Mondon K, Gurny R, Moller M. Novel polymeric micelles for hydrophobic drug delivery based on biodegradable poly(hexyl-substituted lactides). Int J Pharm 2006;319:147—54.
[23] Tian M, Yang Z, Kuwahara K, Nimni ME, Wan C, Han B. Delivery of demineralized bone matrix powder using a thermogelling chitosan carrier. Acta Biomater 2012;8:753—62.
[24] Jiang D, Liang J, Noble PW. Hyaluronan in tissue injury and repair. Annu Rev Cell Dev Biol 2007;23:435—61.
[25] Noble PW. Hyaluronan and its catabolic products in tissue injury and repair. Matrix Biol 2002;21:25—9.
[26] Suzuki K, Anada T, Miyazaki T, Miyatake N, Honda Y, Kishimoto KN, et al. Effect of addition of hyaluronic acids on the osteoconductivity and biodegradability of synthetic octacalcium phosphate. Acta Biomater 2014;10:531—43.
[27] D'Este M, Alini M, Eglin D. Single step synthesis and characterization of thermoresponsive hyaluronan hydrogels. Carbohydr Polym 2012;90:1378—85.
[28] Kumar V, Mostafa S, Kayo MW, Goldberg EP, Derendorf H. HPLC determination of dexamethasone in human plasma and its application to an *in vitro* release study from endovascular stents. Pharmazie 2006;61:908—11.
[29] Bohner M, Baroud G. Injectability of calcium phosphate pastes. Biomaterials 2005;26:1553—63.
[30] Habib M, Baroud G, Gitzhofer F, Bohner M. Mechanisms underlying the limited injectability of hydraulic calcium phosphate paste. Acta Biomater 2008;4:1465—71.
[31] Tadier S, Galea L, Charbonnier B, Baroud G, Bohner M. Phase and size separations occurring during the injection of model pastes composed of beta-tricalcium phosphate powder, glass beads and aqueous solutions. Acta Biomater 2014;10:2259—68.
[32] D'Este M, Eglin D, Alini M. A systematic analysis of DMTMM vs EDC/NHS for ligation of amines to Hyaluronan in water. Carbohydr Polym 2014;108:239—46.
[33] Mortisen D, Peroglio M, Alini M, Eglin D. Tailoring thermoreversible hyaluronan hydrogels by "click" chemistry and RAFT polymerization for cell and drug therapy. Biomacromolecules 2010;11:1261—72.
[34] Bohner M. Design of ceramic-based cements and putties for bone graft substitution. Eur Cell Mater 2010;20:1—12.
[35] Bohner M. Resorbable biomaterials as bone graft substitutes. Mater Today 2010;13:24—30.
[36] Lepperdinger G, Fehrer C, Reitinger S. Biodegradation of hyaluronan. In: Garg HG, Hales CA, editors. Chemistry and biology of hyaluronan. Oxford, UK: Elsevier Science; 2004. p. 71—82.
[37] Bertrand N, Fleischer JG, Wasan KM, Leroux JC. Pharmacokinetics and biodistribution of *N*-isopropylacrylamide copolymers for the design of pH-sensitive liposomes. Biomaterials 2009;30:2598—605.
[38] Pasut G, Veronese FM. State of the art in PEGylation: the great versatility achieved after forty years of research. J Control Release 2012;161:461—72.
[39] Uludag H, D'Augusta D, Golden J, Li J, Timony G, Riedel R, et al. Implantation of recombinant human bone morphogenetic proteins with biomaterial carriers: a correlation between protein pharmacokinetics and osteoinduction in the rat ectopic model. J Biomed Mater Res 2000;50:227—38.
[40] Kirker-Head CA. Potential applications and delivery strategies for bone morphogenetic proteins. Adv Drug Deliv Rev 2000;43:65—92.
[41] McKay B, Sandhu HS. Use of recombinant human bone morphogenetic protein-2 in spinal fusion applications. Spine 2002;27:S66—85.
[42] Welch RD, Jones AL, Bucholz RW, Reinert CM, Tjia JS, Pierce WA, et al. Effect of recombinant human bone morphogenetic protein-2 on fracture healing in a goat tibial fracture model. J Bone Min Res 1998;13:1483—90.
[43] King WJ, Krebsbach PH. Growth factor delivery: how surface interactions modulate release *in vitro* and *in vivo*. Adv Drug Deliv Rev 2012;64:1239—56.
[44] McKay WF, Peckham SM, Badura JM. A comprehensive clinical review of recombinant human bone morphogenetic protein-2 (INFUSE Bone Graft). Int Orthop 2007;31:729—34.
[45] Haidar ZS, Hamdy RC, Tabrizian M. Delivery of recombinant bone morphogenetic proteins for bone regeneration and repair. Part B: delivery systems for BMPs in orthopaedic and craniofacial tissue engineering. Biotechnol Lett 2009;31:1825—35.
[46] Kisiel M, Martino MM, Ventura M, Hubbell JA, Hilborn J, Ossipov DA. Improving the osteogenic potential of BMP-2 with hyaluronic acid hydrogel modified with integrin-specific fibronectin fragment. Biomaterials 2013;34:704—12.
[47] Patterson J, Siew R, Herring SW, Lin AS, Guldberg R, Stayton PS. Hyaluronic acid hydrogels with controlled degradation properties for oriented bone regeneration. Biomaterials 2010;31:6772—81.
[48] Ginebra MP, Traykova T, Planell JA. Calcium phosphate cements as bone drug delivery systems: a review. J Control Release 2006;113:102—10.
[49] Hjerten S, Levin O, Tiselius A. Protein chromatography on calcium phosphate columns. Arch Biochem Biophys 1956;65:132—55.
[50] Hannink G, Geutjes PJ, Daamen WF, Buma P. Evaluation of collagen/heparin coated TCP/HA granules for long-term delivery of BMP-2. J Mater Sci Mater Med 2013;24:325—32.